A Magnetic Transducer Detection System for High Speed Projectiles in Tubes

by

Erik Charles Christofferson

A thesis submitted in partial fulfillment
of the requirements for the degree of

Master of Science
in
Aeronautics and Astronautics

University of Washington

1989

Approved
by_____
(Chairperson of the Supervisory Committee)

Program Authorized
to Offer Degree_____ Aeronautics and Astronautics _____

Date_____

Master's Thesis

In presenting this thesis in partial fulfillment of the requirements for a Master's degree at the University of Washington, I agree that the Library shall make its copies freely available for inspection. I further agree that extensive copying of this thesis is allowable only for scholarly purposes, consistent with "fair use" as prescribed in the U.S. Copyright Law. Any other reproduction for any purposes or by any means shall not be allowed without my written permission.

Signature_____

Date_____

University of Washington

Abstract

A Magnetic Transducer Detection System for High Speed Projectiles in Tubes

By Erik Charles Christofferson

Chairperson of the Supervisory Committee: Professor A. P. Bruckner
Dept. of Aeronautics and Astronautics

A method of chemically accelerating projectiles to hypersonic velocities, the Ram Accelerator, is currently being investigated at the University of Washington. The projectiles are accelerated using a ramjet-in-tube concept. This thesis discusses the design of a system of wall-mounted magnetic transducers used to obtain projectile transit data. Theoretical models for an idealized magnetic transducer are developed to provide a design tool for actual transducer construction. A full description of the system is provided, along with the test fixtures used for the verification of system performance before integration with the experiment. Results of the use of the system in the ram accelerator experiments are included.

TABLE OF CONTENTS

LIST OF FIGURES

NOMENCLATURE

$\vec{A(r)}$	Vector Potential
$\vec{dA}$	Elemental Loop Area
a	Loop Area
$\tilde{a}$	Acceleration
$\vec{B}$	Magnetic Field
d	Radial Distance From Dipole Source to Loop
$\vec{E}$	Electric Field
$\vec{J(r)}$	Current Distribution
J_f	Current Density
$\vec{m}$	Magnetic Dipole Moment
P_n	Legendre Polynomial
t	Time
v_0	Initial Velocity
x	Longitudinal Distance from Dipole Source to Loop
X_s	Skin Depth

Greek Symbols

ϵ	Permittivity
ε_{ind}	Induced Voltage
Φ	Magnetic Flux
μ	Permeability
μ_0	Permeability of Free Space
ρ_f	Charge Density
σ	Conductivity
Θ	Angle (Radians)

Superscripts

$\vec{()}$	Vector Quantity
$\hat{()}$	Unit Vector

ACKNOWLEDGEMENTS

The author wishes to thank various persons for their contributions. Special thanks to Professors A.P. Bruckner and A. Hertzberg for their hands off management style. Professor A.T. Mattick is thanked for his amplifier design and his help in all things electrical. Many thanks go to all of the other research assistants, Carl, Alan, Ed, Peter, Gilbert, etc., whose unrelenting pessimism in the transducer system inspired me to work even harder. Special thanks to Carl Knowlen for many discussions of non-technical matters. Extra-Special thanks to my parents, Dale and Betty, brother Paul and grandmother, Edith. Last but not least, thanks to Christie, just because...

Chapter 1

INTRODUCTION

Theoretical and experimental studies have been performed at the University of Washington on the concept of the ram accelerator, a ramjet-in-tube mass launcher capable of very high velocities. The principle of propulsion of this device is very similar to that of a conventional ramjet. The projectile is initially accelerated with a standard single stage gas gun into a tube filled with high pressure gaseous premixed fuel and oxidizer. The projectile acts as the centerbody of the ramjet while the tube operates as the cowling, (Fig. 1). The flow is compressed supersonically by the diffuser, (projectile nose). The flow is then reduced to subsonic velocities by a normal shock on the aft of the projectile. This shock is stabilized by a thermally choked combustion region at the base of the projectile. Once this process has been initiated and stabilized, the projectile "flies" down the tube, accelerated by the high pressure combustion behind it.

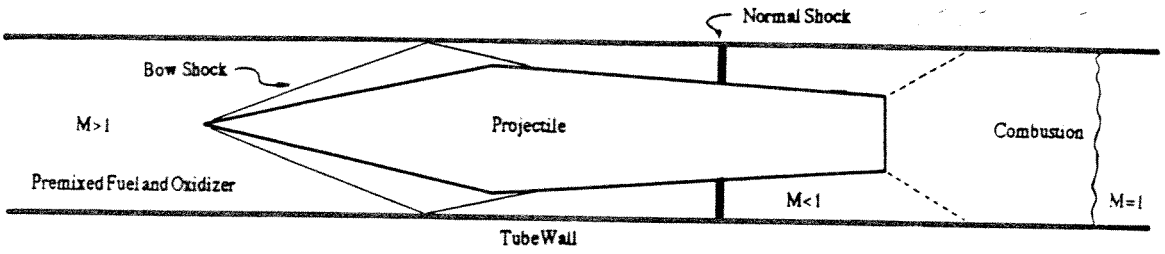

Figure 1 Ram Accelerator Thermally Choked Propulsion Mode

In order to study the operation of the ram accelerator, various types of instrumentation are employed. Currently in use are pressure, optical and magnetic transducers. The pressure and optical transducers can be used to determine position, velocity and accelerations of the projectile, but not to a reasonable degree of accuracy. The pressure and luminosity waveforms vary greatly at different points throughout the tube. These variations can occur from the changes in Mach number during transit or from changes in fuel and oxidizer mix in various experiments. This makes determining the location of the projectile in relation to the data inaccurate. A method is required to

consistently and unambiguously determine the position of the projectile in the tube as a function of time to correlate it with the pressure and light emission data. This requirement is fulfilled by the magnetic transducer system.

The magnetic transducer is essentially a loop of wire placed in the ram accelerator tube wall. If a magnetic field passes by the loop an electrical current will be generated in the loop. To provide a magnetic field one or two magnets are placed in a projectile at the throat (the longitudinal location of projectile maximal cross-section area), and/or tail (Fig. 2). When a projectile passes a transducer a waveform characteristic of the projectiles' magnet orientation can be monitored. This provides accurate transit data which can be matched with pressure or optical data if transducers are located at the same station (longitudinal position) on the tube. This allows for a better understanding of various phenomena by attaching a projectile position in relation to the luminosity and pressure traces (Fig. 3).

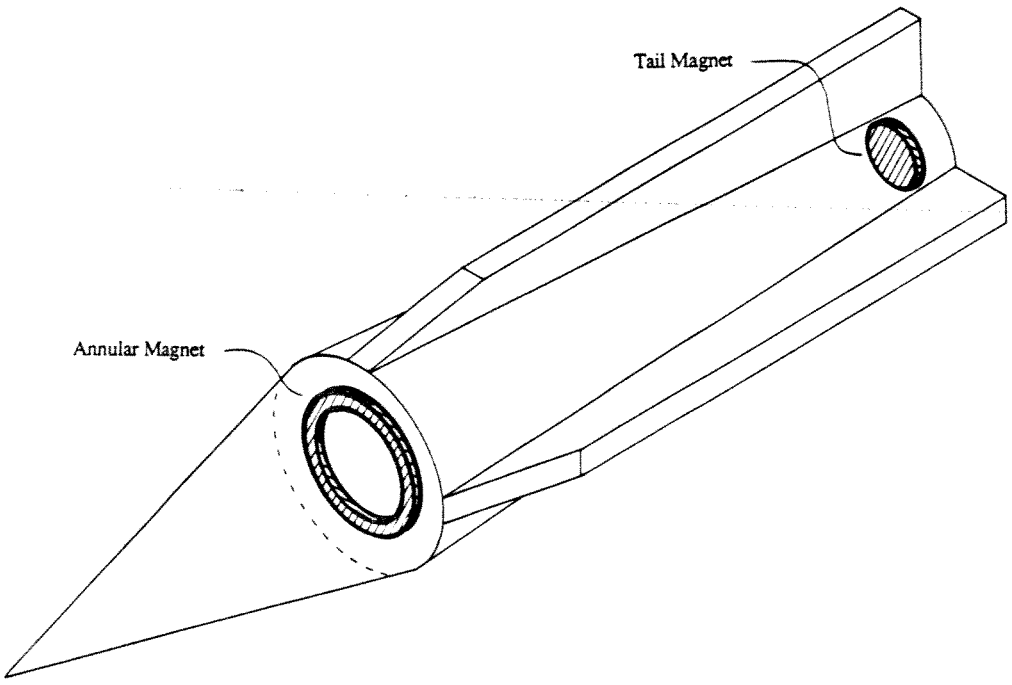

Figure 2 Magnet Positions in Projectile

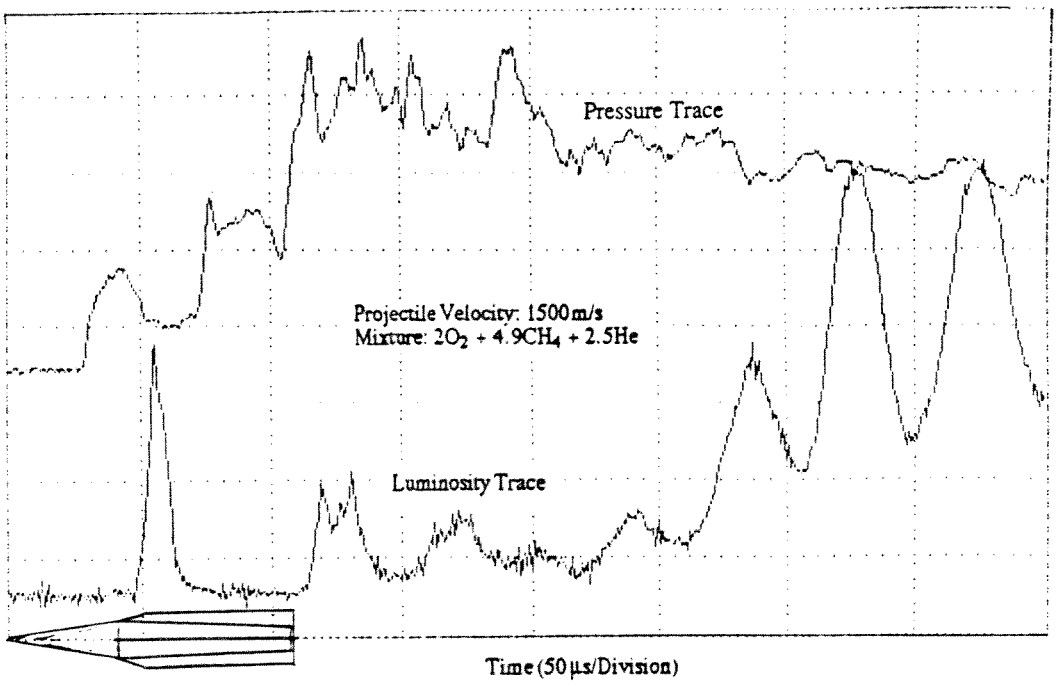

Figure 3 Relation of Projectile Position to Data

The magnetic transducers are also used to determine velocity and acceleration. The ram accelerator tube has instrument ports at various locations down its length, (Fig. 4). By taking the time difference between the projectile passage at two successive locations, and knowing the transducers separation distance, a mean velocity can be calculated. Successive velocities can be used to find mean accelerations.

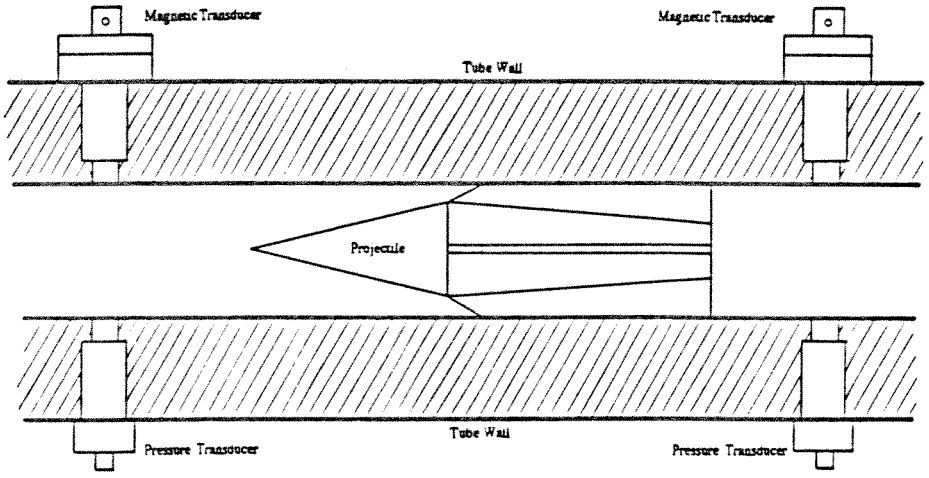

Figure 4 Relation of Projectile to Transducers in Tube

Chapter 2

THEORY

The starting point at which to examine the transducer system is the structure of the magnetic field, $\vec{B}$. From this the voltage induced in the magnetic transducer can be derived from Faraday's law. To begin, a vector potential $\overrightarrow{A(r)}$ is assumed for a current distribution, $\overrightarrow{J(r)}$, in some volume V, (Fig. 5). (This vector potential allows the structure of the magnetic field to be found. The magnetic field is equal to the curl of the vector potential).

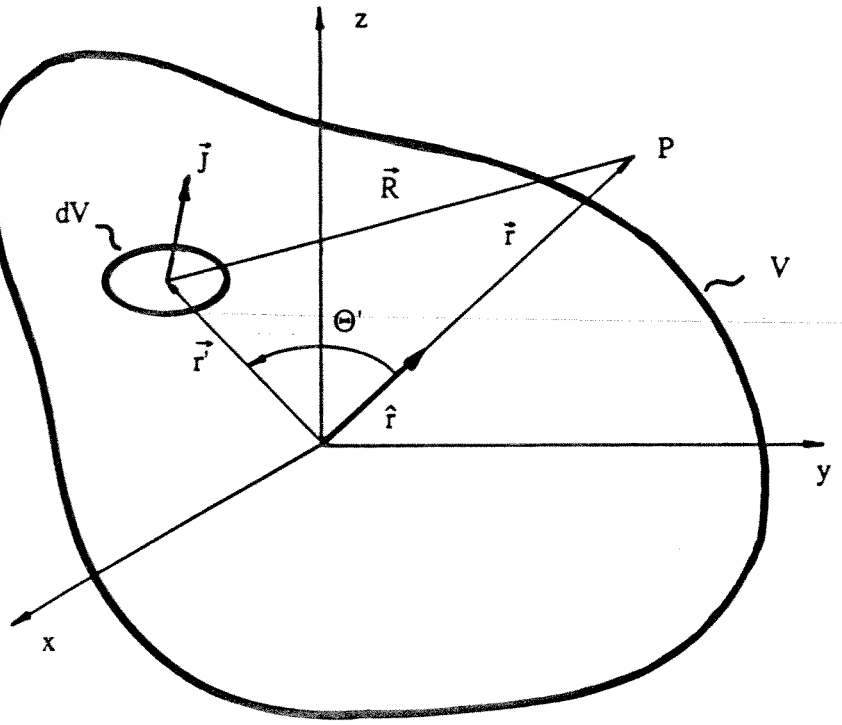

Figure 5 Vector Potential

$$\overrightarrow{A(\vec{r})}=\frac{\mu_0}{4\pi}\int \frac{J(\vec{r}')dV}{|\vec{r}-\vec{r}'|} \qquad (1)$$

Through a Legendre polynomial expansion this integral can be written as an infinite series:

$$\overrightarrow{A(\vec{r})}=\frac{\mu_0}{4\pi}\sum_{n=1}^{\infty}\frac{1}{r^{n+1}}J(\vec{r'})\,\vec{r'}^{n}P_n(\cos\Theta')\,dV \tag{2}$$

$$\overrightarrow{A(\vec{r})}=\vec{A}_0+\vec{A}_1+\vec{A}_2+\vec{A}_3+\ldots \tag{3}$$

The first term to examine is the A_0 term for the lowest order effects. A_0 is proportional to $1/r$, A_1 is proportional to $1/r^2$, A_3 to $1/r^3$, etc.. It can be shown that the A_0 term is zero due to the integrated current distribution being zero, (see Reference 5). Physically this corresponds to the monopole term of the vector potential expansion and, thus, would be expected to be zero.

The second term, A_1, is the dipole term, and is

$$\overrightarrow{A_1(\vec{r})}=\frac{\mu_0}{4\pi r^2}\int J(\vec{r'})(\hat{r}\cdot\vec{r'})dV \tag{4}$$

With the use of vector identities this can be written as

$$\overrightarrow{A_1(\vec{r})}=\frac{\mu_0}{4\pi r^2}\frac{1}{2}\int(\vec{r'}\times J(\vec{r'})dV)\times\hat{r} \tag{5}$$

For convenience, define the magnetic dipole moment, $\vec{m}$.

$$\vec{m}=\frac{1}{2}\int(\vec{r'}\times J(\vec{r'}))dV \tag{6}$$

Therefore the vector potential can now be written in its final form

$$\overrightarrow{A_1(\vec{r})}=\frac{\mu_0}{4\pi r^2}\vec{m}\times\hat{r} \tag{7}$$

$$\overrightarrow{A_1(\vec{r})}=\frac{\mu_0}{4\pi}\frac{\vec{m}\times\vec{r}}{r^3} \tag{8}$$

The actual magnetic field can be derived from the vector potential by

$$\vec{B} = \nabla \times \vec{A} \tag{9}$$

At this point the assumption will be made that the higher order terms, A_2,A_3, etc. , can be neglected. As was previously mentioned A_n is proportional to $1/r^{(n+1)}$, therefore terms of higher order will be much smaller and can be neglected. Thus, a perfect dipole field will be used for the magnetic field source. This is a standard practice when dealing with magnetic fields. The magnetic field can then be written as

$$\vec{B} = \nabla \times \frac{\mu_0}{4\pi} \frac{\vec{m} \times \vec{r}}{r^3} \tag{10}$$

Taking the constants outside of the curl operator

$$\vec{B} = \frac{\mu_0}{4\pi r^3} (\nabla \times (\vec{m} \times \vec{r})) \tag{11}$$

By vector identities the final expression for the magnetic dipole field is

$$\vec{B} = \frac{\mu_0}{4\pi r^3} (3(\vec{m} \cdot \hat{r})\hat{r} - \vec{m}) \tag{12}$$

The transducer to be used is ideally modeled as a simple circular loop of wire. By using Faraday's law the voltage induced in the loop can be found.

$$\varepsilon_{ind} = - \frac{\partial \Phi}{\partial t} \tag{13}$$

Where Φ is the magnetic flux through the loop:

$$\Phi = \int \vec{B} \cdot \, d\vec{A} \tag{14}$$

Now the geometry of the actual problem must be included, (see Fig. 6).

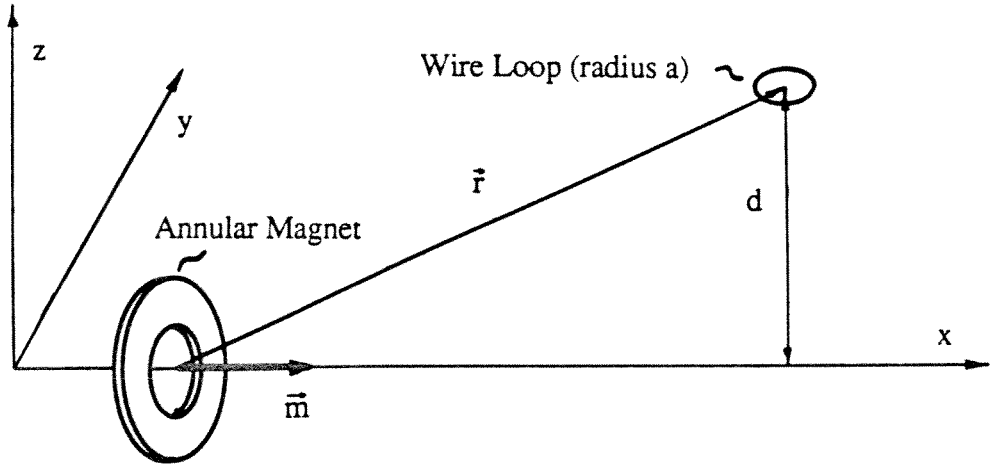

Figure 6 Magnet to Loop Geometry

$$\vec{m} = m\hat{x} \tag{15}$$

$$\vec{r} = x\hat{x} + d\hat{z} \tag{16}$$

$$\hat{r} = \frac{x\hat{x} + d\hat{z}}{(x^2 + d^2)^{\frac{1}{2}}} \tag{17}$$

By substitution the magnetic field can now be written for this particular geometry.

$$\vec{B} = \frac{\mu_0}{4\pi}\left(\frac{3(mx^2\hat{x} + mxd\hat{z})}{(x^2 + d^2)^{\frac{5}{2}}} - \frac{m\hat{x}}{(x^2 + d^2)^{\frac{3}{2}}}\right) \tag{18}$$

By examining Faraday's law it is seen that only magnetic field components that pass through the loop contributes to the induced voltage. From Fig. 6 it can be seen that this requires only the component of the magnetic field in the z direction to be kept.

$$\vec{B}_z = \frac{\mu_0}{4\pi}\left(\frac{3mxdz)}{(x^2 + d^2)^{\frac{5}{2}}}\right)\hat{z} \tag{19}$$

If it is assumed that the loop is small enough so that the field strength within it can be considered to be constant, then the flux can be written as

$$\Phi = \left(\frac{a^2\mu_0 3mxdz)}{4(x^2 + d^2)^{\frac{5}{2}}}\right) \tag{20}$$

In the acquisition of data in the ram accelerator experiment, information is referenced in time (t), not location (x). Therefore the following substitutions are made:

$$x = v_0 t + \frac{1}{2}\tilde{a}t^2 \tag{21}$$

$$\gamma = \frac{a^2\mu_0 3md}{4} \tag{22}$$

For simplicity a zero acceleration state is assumed and thus the flux can be expressed as:

$$\Phi = \frac{\gamma v_0 t}{(v_0^2 t^2 + d^2)^{\frac{5}{2}}} \tag{23}$$

The induced voltage is found by taking the negative of the derivative of the flux with respect to time, (Eq. 13).

$$\varepsilon_{ind} = -\frac{\partial}{\partial t}\left[\frac{\gamma v_0 t}{(v_0^2 t^2 + d^2)^{\frac{5}{2}}}\right] \tag{24}$$

$$\varepsilon_{ind} = \left[\frac{\gamma v_0}{(v_0^2 t^2 + d^2)^{\frac{5}{2}}}\right]\left[1 - \frac{5v_0 t^2}{(v_0^2 t^2 + d^2)}\right] \tag{25}$$

This will give an idealized look at the character of the signal from a perfect dipole magnetic source as seen by a single loop of wire. A further unstated assumption has been that there is no attenuation or phase shift of the B field flux due to a conductive medium between the wire loop and magnetic dipole source. A transducer used in the ram accelerator sees very large heat and pressure pulses and consequently requires a protective covering over the fragile wire loops, (in actual probe construction, multiple wire loops are used and will be examined in later chapters). For analysis the problem of phase shift and attenuation is stated as that of plane waves traveling in a conductive medium. (The conductive media is a stainless steel casing that protects the loops from the thermal and pressure pulses).

To begin the analysis a linear isotropic homogeneous conducting medium, (stainless steel, the material used in the transducer casing construction), is assumed to surround the loop. For this case Maxwell's equations reduce to:

$$\nabla \cdot \vec{E} = \frac{\rho_f}{\epsilon} \tag{26}$$

$$\nabla \times \vec{E} = -\frac{\partial \vec{B}}{\partial t} \tag{27}$$

$$\nabla \times \vec{B} = \mu\sigma\vec{E} + \mu\vec{J}_f + \mu\epsilon\frac{\partial \vec{E}}{\partial t} \tag{28}$$

Assuming there are no external free charges, i.e., $\rho_f = J_f = 0$, these equations reduce to:

$$\nabla \cdot \vec{E} = 0 \tag{29}$$

$$\nabla \times \vec{B} = \mu\sigma\vec{E} + \mu\epsilon\frac{\partial \vec{E}}{\partial t} \tag{30}$$

$$\nabla \cdot \vec{B} = 0 \tag{31}$$

Taking the curl of $\nabla \times \vec{B}$

$$\nabla \times (\nabla \times \vec{B}) = \nabla(\nabla \cdot \vec{B}) - \nabla^2 \vec{B} = -\nabla^2 \vec{B} \tag{32}$$

$$= \mu\sigma(\nabla \times \vec{E}) + \mu\epsilon \frac{\partial}{\partial t}(\nabla \times \vec{E}) \tag{33}$$

$$= -\mu\sigma \frac{\partial \vec{B}}{\partial t} - \mu\epsilon \frac{\partial^2 \vec{B}}{\partial t^2} \tag{34}$$

In the ram accelerator the tube wall acts like an infinite steel plate. This conductive medium, when a loop inside a stainless steel case is placed in the tube wall, separates the loop from the dipole by the equivalent of an infinite conductive plate. This is analogous to a 1-D geometry. Thus, Eq. 34 can be used in 1-D form:

$$\frac{\partial^2 \vec{B}}{\partial x^2} = -\mu\sigma \frac{\partial \vec{B}}{\partial t} - \mu\epsilon \frac{\partial^2 \vec{B}}{\partial t^2} \tag{35}$$

This is the standard 1-D wave equation with the inclusion of a dissipation term. It is easily solved by the method of separation of variables, yielding:

$$\vec{B} = B_0 e^{-\beta x} e^{i(\alpha x - \omega t)} \tag{36}$$

$$\beta = \omega\left(\frac{\mu\epsilon}{2}\right)^{\frac{1}{2}} \left(\left(1 + \left(\frac{\sigma}{\omega\epsilon}\right)^2\right)^{\frac{1}{2}} - 1 \right)^{\frac{1}{2}} \tag{37}$$

$$\alpha = \omega\left(\frac{\mu\epsilon}{2}\right)^{\frac{1}{2}} \left(\left(1 + \left(\frac{\sigma}{\omega\epsilon}\right)^2\right)^{\frac{1}{2}} + 1 \right)^{\frac{1}{2}} \tag{38}$$

The value of β gives the attenuation of the wave through the media. The point at which the amplitude of the magnetic field decays by a factor of 1/e is known as the skin depth, X_S.

$$X_s = \frac{1}{\beta} \tag{39}$$

The value of α describes the amount of phase shift, or signal lag, through unit thickness of medium. By taking the product of α and the thickness of the material that has been penetrated, the phase shift can be calculated.

In modeling the magnetic transducer system the magnetic field was approximated as a perfect dipole source, and the transducer was assumed to consist of a single loop of wire. As previously mentioned, the actual transducers use multiple wire loops. This creates a complex geometry between the dipole source and the loops which does not allow for a closed form solution. This situation is readily handled by use of numerical techniques in a computer code.

The magnetic source used in the ram accelerator is an annulus of magnetic material. This annulus can be looked at as an infinite number of dipole source, (Fig. 7). By examining the equation for the induced voltage and the relative geometry of the annulus to the transducer, some conclusions can be drawn. The factor that affects the induced voltage is the radial distance from transducer coil to annulus, (the longitudinal distance is constant over the annulus).

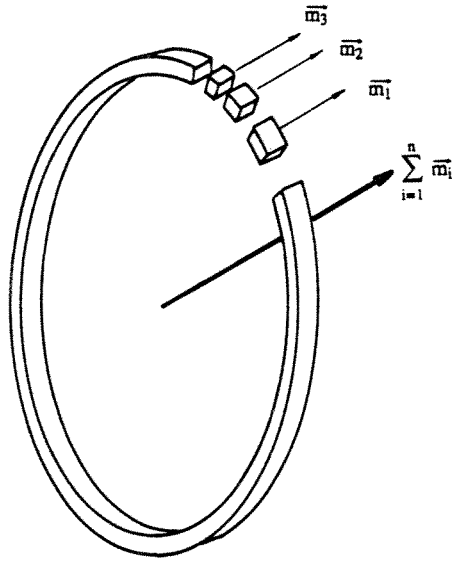

Figure 7 Annular Magnet as a Sum of Dipoles

$$\varepsilon_{ind} \sim \frac{1}{d^4} \tag{40}$$

This gives the result that the collection of dipole sources act additively with respect to the induced voltage. This collection of dipole sources can also be effectively summed into an overall dipole source strength, $\vec{m}$. This is what is done to simplify the construction of the numerical model used in the computer code.

The code allows for the inclusion of possible effects disregarded in previous derivations. The first of these is in the use of multiple loops. The actual transducers use multiple loops and each loop is treated as a single entity that is wired in series to successive loops. This requires an iterative process to find the induced voltage of each loop and then sum the output voltage of all loops. Another prior assumption required the flux through a loop to be constant at all points in the loop, to allow for a closed form solution for a single loop. In the code the interior of the wire loop is broken up into strips. The flux through each strip is calculated and summed over the loop. This provides a more accurate value for the induced voltage than with the closed form solution. By reducing the number of assumptions used in the model of the system, and numerically calculating the results in a computer code, a more accurate description of the system is obtained.

Chapter 3

EXPERIMENTAL APPARATUS

The magnetic transducer system consists of two main components, the transducer itself and an amplifier. To verify the system performance before integrating it with the ram accelerator two test fixtures were built. Each of these items are examined in turn.

The magnetic transducer is built in two pieces, the bobbin and the casing, (Fig. 8). The casing is made of 304 stainless steel. Stainless steel is used because of its high strength as a non-ferrous material. (A non-ferrous material is required to insure that the casing does not become magnetized). Its purpose is to protect the bobbin from the high pressure (~20,000 psi) and high temperature (2000-3000°K) enviorment in the ram accelerator. Various modes of failure were examined for the casing geometry. It was determine that shearing of the tip of the casing, the so called cookie cutter failure (Fig. 9), was the limiting case of failure. This gave a minimum casing tip thickness of .060 in. . An O-ring is also included on the seal between the casing and the ram accelerator tube to prevent leakage of the high pressure gas in the tube.

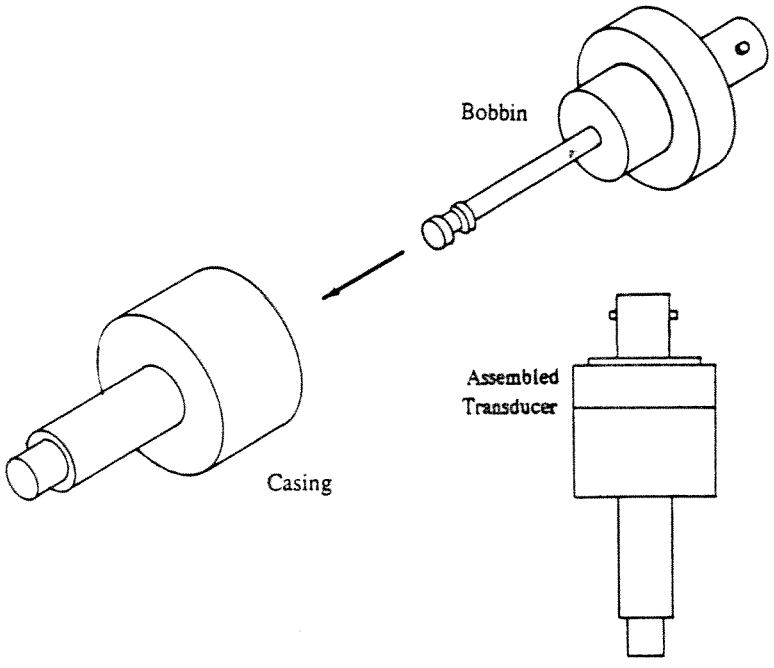

Figure 8 Bobbin and Casing

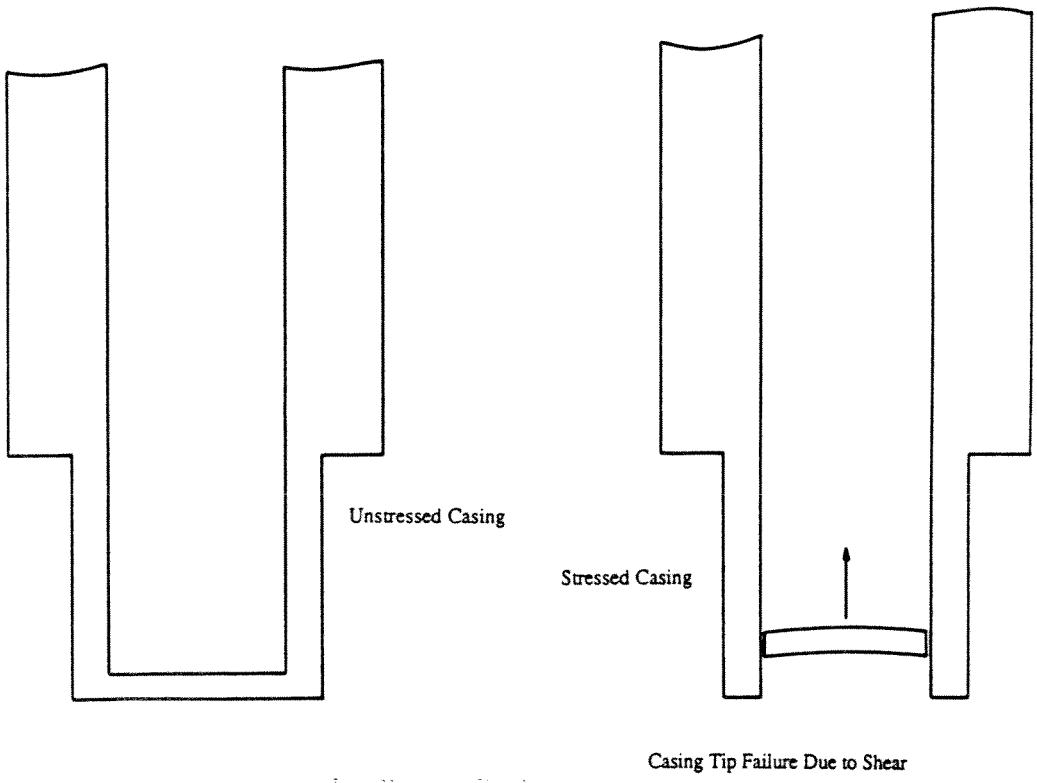

Figure 9 Cookie Cutter Failure

The bobbin with its associated components, is the actual sensing element of the transducer, (Fig. 10). The bobbin itself is made of Lexan, (polycarbonate). This material was chosen because it is a dielectric, is easy to machine, and is strong. A length of 40HF magnet wire was used to create approximately 40 loops around the bobbin tip. The ends of the wire are fed through two small holes in the top of the bobbin and soldered to a standard BNC plug. The wire loops are potted in paraffin wax to prevent movement of the loops and possible resultant damage. The BNC plug is attached to the bobbin with machine screws. The entire bobbin assembly is inserted into the casing and secured with machine screws, as in Fig. 8.

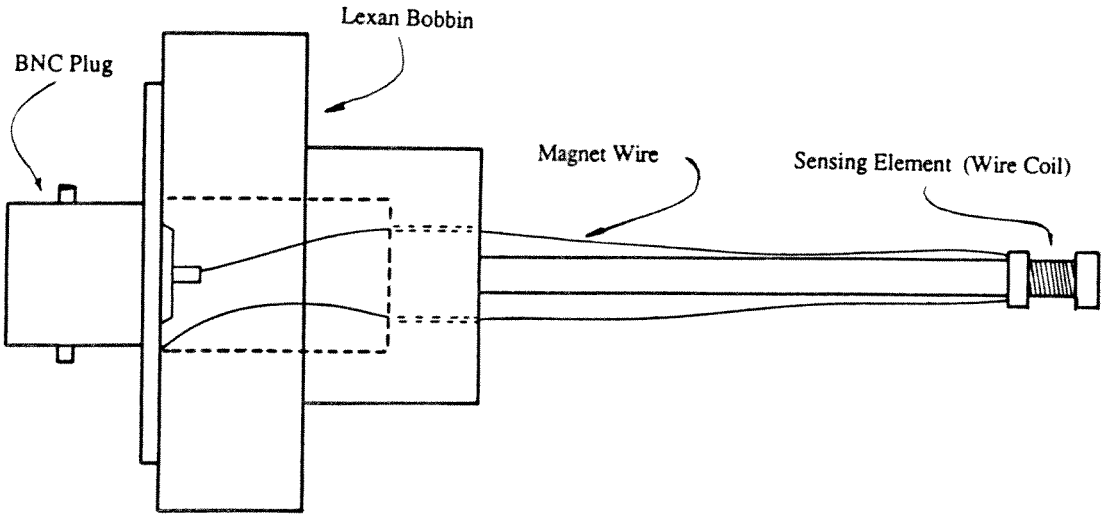

Figure 10 Bobbin

This particular transducer arrangement offers advantages over previous designs (see Reference 3). The sensing element is never in contact with high pressure and high temperature gas, since the casing isolates the sensing element and takes all temperature and pressure loadings. In the event of a transducer sensor failure, an entire rebuild can be achieved in a matter of minutes, or an extra bobbin can be put into a casing without the casing having to be removed from the tube.

The other major component of the system is the amplifier. The small pulse width and low output of the transducer requires a high gain-bandwidth amplifier, (Fig. 11), (the magnetic pulse was found to generate an equivalent frequency of 67 kHz for a projectile velocity of 2 km/sec). The ram accelerator's data acquisition system (DAS) samples at a rate of 1 MHz. By setting the bandwidth of the amplifier at a larger value than that of the DAS, an accurate record of the transducer's output can be assured within the limits of the DAS. This is achieved by cascading two operational amplifiers. (These are type LM359 which is a dual Op-Amp). The amplified signal is then run through a line driver, (LH0002CN), to ensure that a signal is cleanly propagated over possibly long cable lengths to the DAS. This amplifier ideally provides a bandwidth of 2 MHz with a gain of 800.

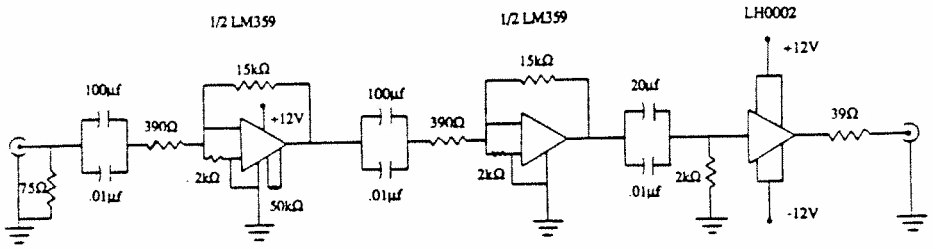

Figure 11 Amplifier Schematic

The ram accelerator is fired, on average, four times per week. There are a very limited number of DAS channels available. These two factors make pre-testing the system very desirable. To allow for a system check, two bench test devices were constructed. These are the phase shift and low speed output test rigs.

The phase shift test rig consists of multiple loops of magnet wire around a ferromagnetic steel rod with the wires attached to a Hewlett Packard 3311A function generator, (Fig. 12). The output of the function generator is set to maximum and the frequency is set to the previously mentioned 67 kHz. The current pulsing through the loops at the end of the steel rod produces a magnetic field oscillating at the frequency characteristic of the magnet in the ram accelerator projectile as it passes the transducer. This allows for the testing of a bare coil and a capped coil to determine phase shift.

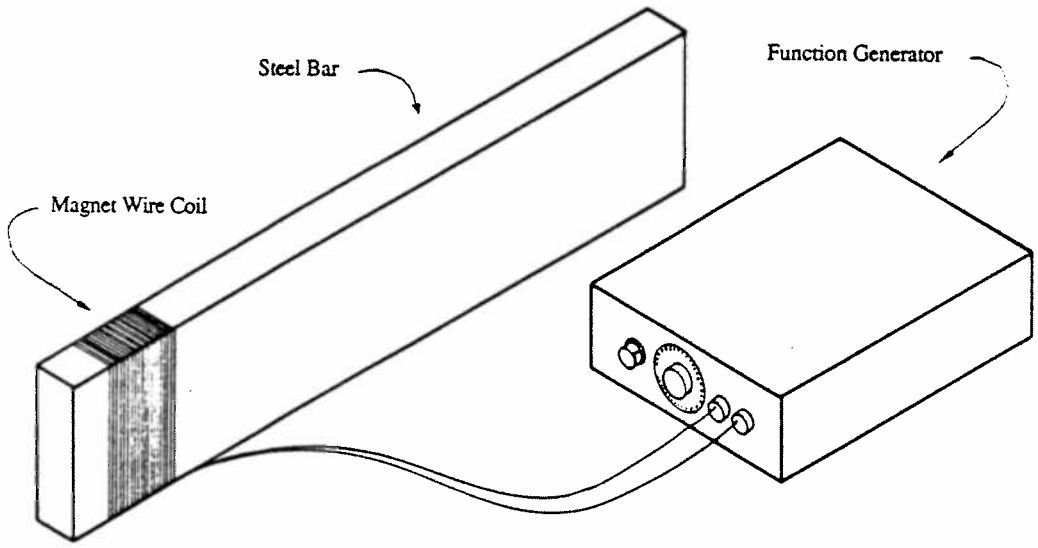

Figure 12 Phase Shift Test Rig

To test the transducer's output with or without an amplifier, a low speed test rig was constructed, (Fig. 13). This unit simulates the transducer to annular magnet geometry of the ram accelerator at low velocities. A standard projectile magnet is attach to a magnesium disk. This disk is connected by a threaded rod to a hub. A counter balance disk is attached to the opposite side of the hub. The hub assembly is attached to a 110 volt AC motor whose rotation rate is controlled by a Staco 3PN 501 variac. The motor assembly is bolted to a piece of plywood with rubber feet to dampen vibrations from inevitable unbalances in the hub assembly. A steel plate, (4150), is bolted next to the motor. The plate is drilled and tapped to accept a magnetic transducer. The plate simulates the tube wall in which the transducer is mounted.

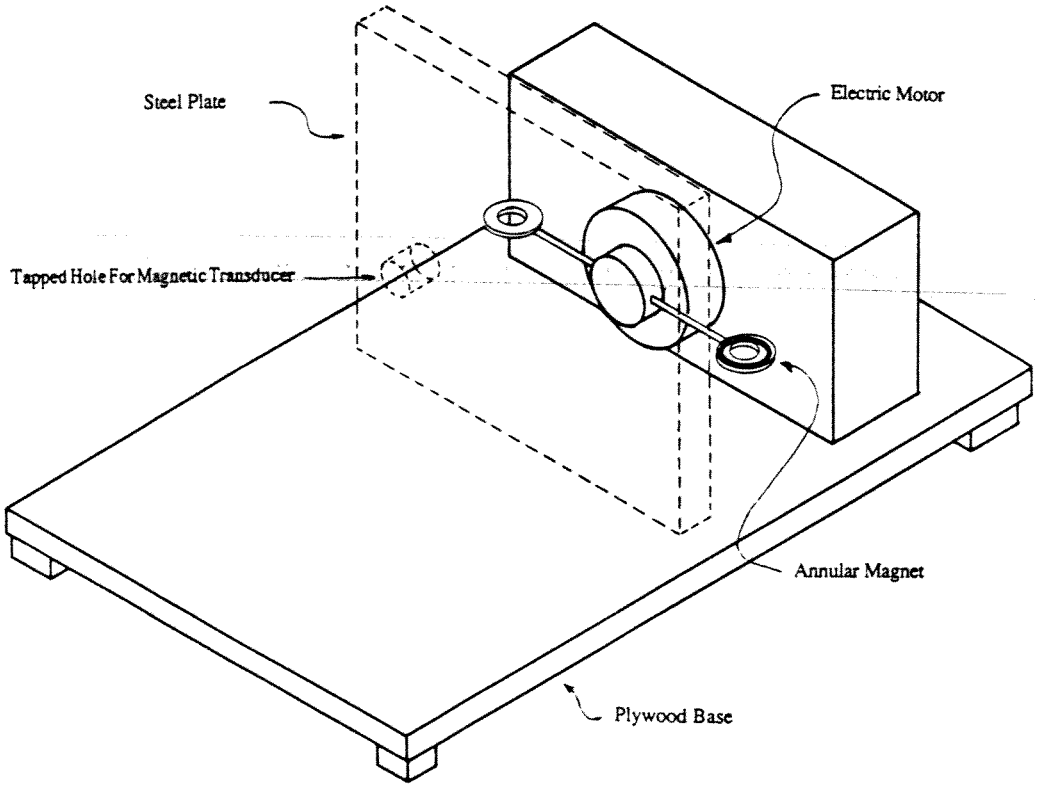

Figure 13 Low Speed Test Rig

Chapter 4

RESULTS

By examining the solution of the wave equation (Eq. 36), two areas of interest can be explored, the skin depth and the phase shift through the stainless steel casing tip. These values are determined by the parameters α and β, (Eq. 38 and 37). If polarization and a free flow of electrons in the casing are neglected, the permeability and permittivity of free space may be used. This is a reasonable approximation in that neither value would vary by more than a percent under normal conditions, (see Reference 5). The conductivity of the stainless steel is readily available from materials handbooks. A pulse width of 35 μs is equivalent to a circular frequency of 180 kHz. This results in a skin depth of .16 in. and a phase shift of 31°. For a single pulse a phase shift manifests itself as a time delay. For the equivalent pulse frequency used, the theory predicts a time delay of 3 μs. The casing tip thickness is .06 in. for the structural reasons mentioned earlier. Since the skin depth is much greater than this, the pulse strength will not be attenuated to a large degree. Theory predicts that the signal strength will retain 70% of it original magnitude.

The experimental results agree well with the theory for the time delay. Fig. 14 shows the result of the bench test. The function generator supplied a 35 μs sinusoidal pulse to the test rig coil. Two magnetic transducers, one with its casing in place, the other using only the uncased bobbin, were placed side by side next to the test rig coil. It can be seen that the wave crest of the capped transducer lags 5 microseconds behind that of the uncapped transducer.

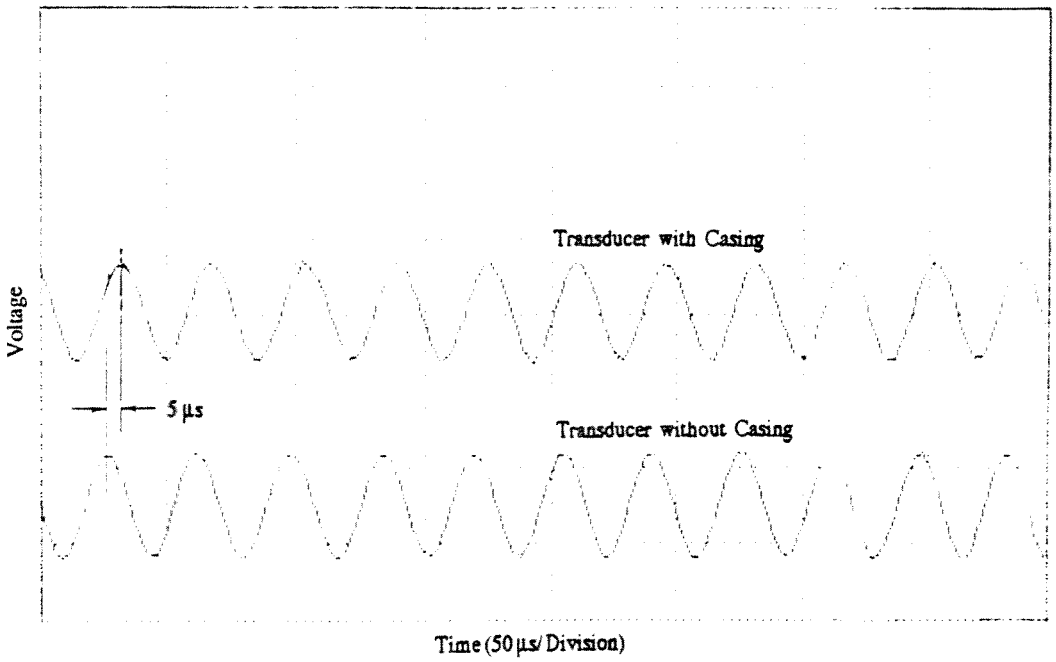

Figure 14 Test Rig Output for Phase Shift

A final test for the phase shift was conducted during an actual ram accelerator shot, (Fig. 15). (Unfortunately only low bandwidth amplifiers were available at the time of the test. This resulted in the signal traces being integrated, however integration does not change the relative phase shift between the traces, thus this does not prevent the determination of the time delay). One transducer was installed in the tube with no protective tip casing, the other was in a standard cased configuration. It can be seen that the time delay is 2 µs. This agrees well with the theoretical value of 3 µs.

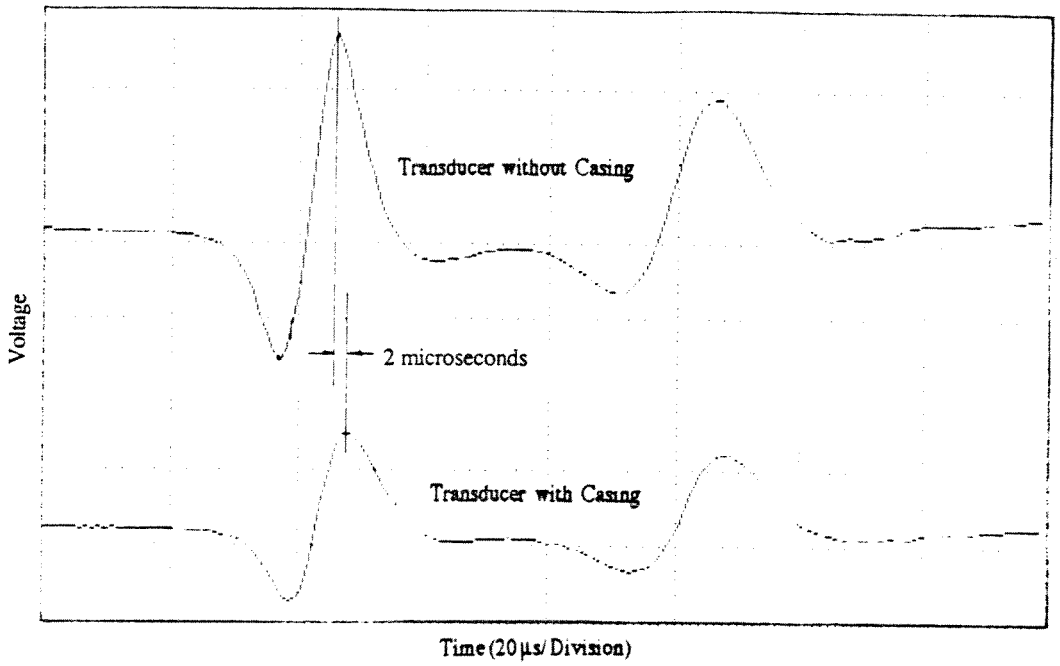

Figure 15 Ram Accelerator Phase Shift Test

The error of 1 μs between the ram accelerator shot data and the theory is at the limit of the resolution of the DAS. Thus, the agreement is excellent. The bench test results do not match as well. The theory was derived for a plane wave,a 1-dimensional problem. The transducers in the ram accelerator tube do see essentially a 1-D wave, but the test rig transducers do not. The test rig transducers were not embedded in a conductive medium that effectively would shield them from 3-D effects. (These effects were neglected in the solution derived for the theory). This lack of shielding allows for the 3-D effects to influence the delay and cause the error between the theory and experiment.

The validity of the computer code was verified by using the low speed test rig. This also allowed for an empirical determination of the magnetic dipole moment, $\vec{m}$. Fig. 16 shows the pulse generated by the test rig. The radius of the magnetic ring on the test rig is known, 4.7 cm. By measuring the time from pulse to pulse a linear velocity for the magnet is found. The pulse shown is for a magnet velocity of 26.8 m/s. This waveform is characteristic of a quadrupole. Characteristic values that should be noted are the pulse width and the ratio of maximum to minimum amplitude. (The maximum amplitude is the positive voltage peak, while the minimum amplitude is the maximum negative voltage

peak). The pulse width is defined as the time difference from the first voltage maximum to the second. For this case it is approximately 650 μs. The amplitude ratio is .275.

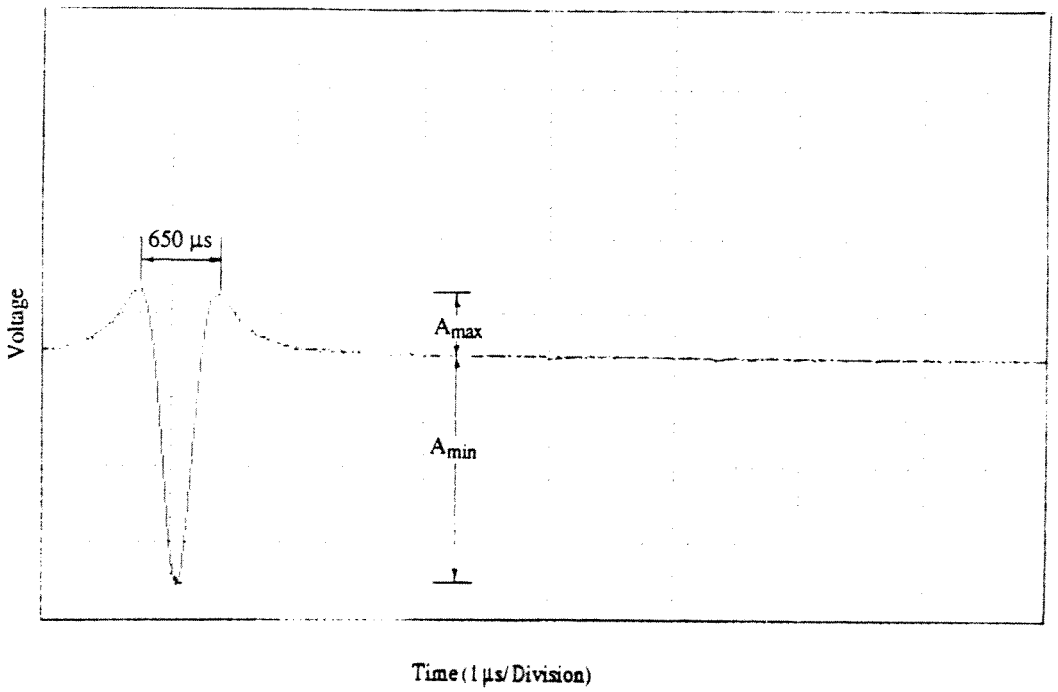

Figure 16 Low Speed Test Output

Fig. 17 shows the computer simulation of the test rig pulse. The code was supplied with magnet velocity and transducer to magnet geometry. It is seen that the appropriate quadrupole waveform is produced. A pulse width of 450 μs and an amplitude ratio of .308 is found. The amplitude ratio error between the test rig and computer code is 11%.This error can be attributed to the finite steps in the computer code. The voltage is proportional to rate of change of the magnetic field with respect to time. By taking a coarser or finer grid, (in time), with the computer code, the amplitude ratio is varied. A coarse grid (200-400 grid points) will tend to integrate the pulse , thus providing erroneous data. A finer grid will be a closer approximation to the continuum as sampled by the DAS. An 11% error is considered acceptable for design purposes, (a higher grid resolution required excessive CPU time, the grid used was comprised of 1000 grid points).

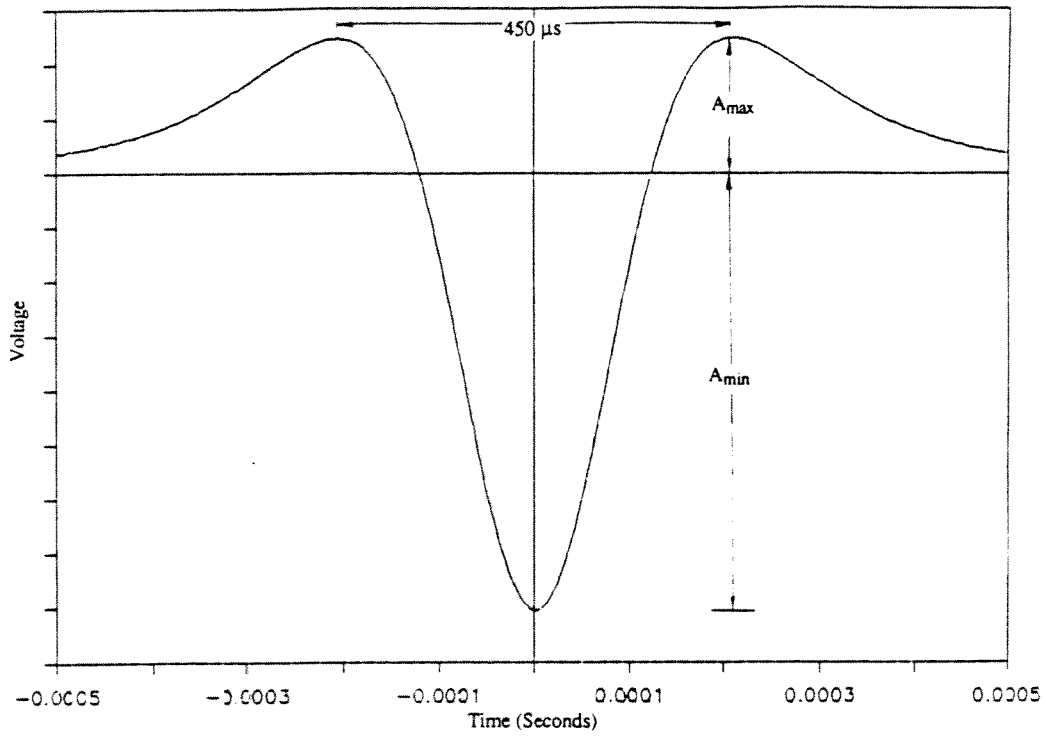

Figure 17 Computer Simulation of Low Speed Test

The pulse width had an error of 30% between theory and test rig experiment. This error stems from the fact that the computer code models the magnet traveling in a straight path. The test rig moves the magnet in circles, thus the magnet passes the transducer in an arc. This means that at a given linear velocity the magnet spends a longer time in the vicinity of the transducer. The actual magnet path on the test rig, by staying near the transducer longer, produces a wider pulse width as is observed.

The magnetics data from a ram accelerator experiment are shown in Fig. 18. Using the correct geometry, velocity and acceleration, the computer code produced the output in Fig. 19. The pulse width and amplitude ratio are found to be 46 μs and 0.39 for the experiment. Corresponding values of 40 μs and 0.29 are produced by the computer code. The pulse width error is 10%. This is a large reduction from the 30% error in the low speed case, but it cannot be accounted for by possible errors in taking physical measurements. If equation 25 is non-dimensionalized it can be shown that the pulse width is:

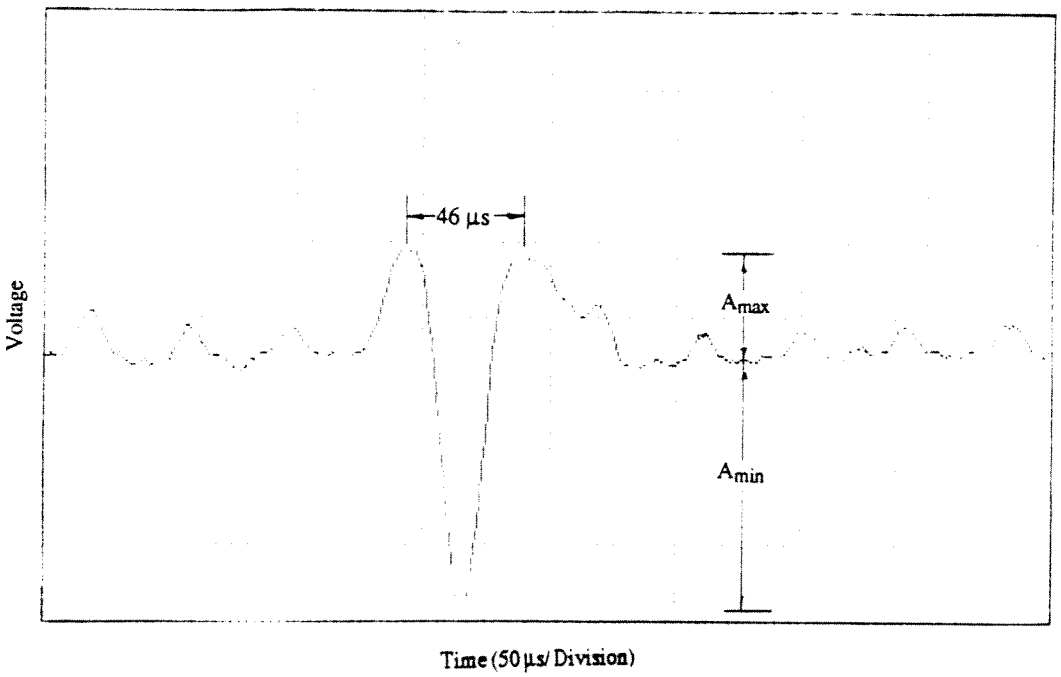

Figure 18 Ram Accelerator High Speed Data

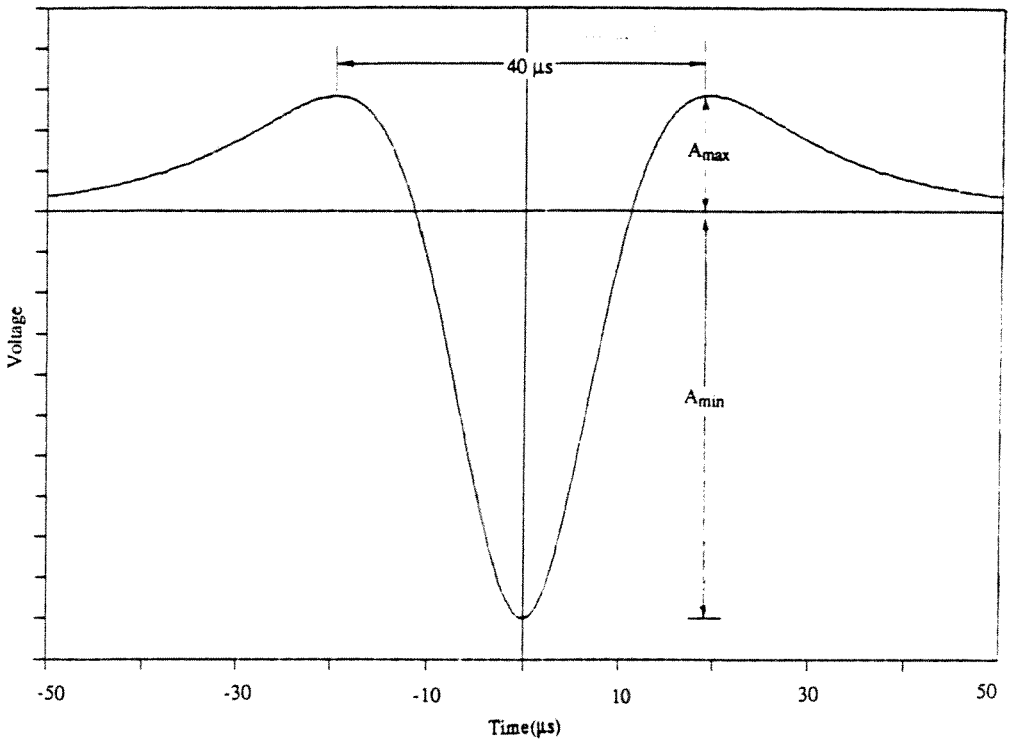

Figure 19 Computer Simulation of High Speed Data

$$\Delta t = \sqrt{3}\frac{d}{v}$$

The velocity of the magnet is well defined, however the radial distance from the transducer to the magnetic dipole is less well defined. In the model it was assumed that the annular magnet could be approximated by a single dipole source located at the tube center. It is clear that the actual magnet geometry would need to be incorporated into the model to achieve more accurate results. It should be stated that the purpose of the code is to allow for a transducer design to be tested numerically before its actual physical construction. For the ram accelerator experiments the 10% error in the output of the computer code is acceptable for design purposes. The error in the amplitude ratio is 25%. This is found to be somewhat ambiguous due to the noise on the experimental signal, i.e the zero voltage point is not well defined. However, the same argument for the coarseness of the computer code's time resolution could explain possible error.

By examining the the equations used in the model some valuable design information can be found. From Eq. 25 the maximum absolute value of the voltage is given by:

$$[\varepsilon_{ind}]_{max} = \frac{3a^2\mu_0 m v_0}{4d^4}$$

Even though this is for an idealized single wire loop and perfect dipole source, all of the relationships hold true for the more complex transducers used in experiments. It is evident that the primary parameters that would have the greatest effect are the loop radius, a, and the radial distance from the the loop to the magnet, d. These values were maximized and minimized, a and d, respectively, for the transducers built, (within the limits imposed by instrument ports in the tube and by structural considerations).

The magnetic transducers are used for projectile location, velocity and acceleration data acquisition. The ram accelerator tube has instrument ports at various locations down its length. By taking the time difference between the projectile passage at two successive locations, and knowing the magnets' separation distance, a mean velocity can be calculated. Successive velocities can be used to find mean accelerations.

Unfortunately this method only gives the mean values over the length of tube between two transducers. A new method is currently being used to find velocities at a single transducer. This is achieved by installing a magnet at the aft end of the projectile, as

well as the annular magnet , as shown in Fig. 1. This allows for the time difference between the two magnets at a single transducer to be used, along with the magnet separation distance, to find velocity. This does not result in a more accurate determination of accelerations, but does produce the value of the projectile's instantaneous velocity with more accuracy than the two-transducer approach.

Chapter 5

CONCLUSION

A magnetic transducer system for the detection of high speed projectiles in tubes was presented. The theory governing the operation of the idealized transducers was developed from basic principles. A computer code with the ability to approximate the actual, non-ideal, transducers was explained. The transducer system components as well as the necessary test rigs for system validation were described.

The results of experiments with the test rigs were compared to the computer code and found to agree fairly well. The actual ram accelerator experimental data were found to agree very well with the code. Methods of velocity and acceleration measurements were discussed for use with multiple transducers. A single transducer velocity measurement was also discussed.

Use of the magnetic transducer system for velocity measurements has been validated. By use of a computer code simulation and closed form solutions of the transducer system, useful design tools have been developed to optimize the transducer system design.

LIST OF REFERENCES

1. Hertzberg, A., Bruckner,A.P., and Bogdanoff, D.W., "Ram Accelerator: A New Chemical Method for Accelerating Projectiles to Ultrahigh Velocities," AIAA Journal, vol. 26, Feb. 1988 pp. 195-205.

2. Bruckner, A.P., Knowlen, C., Scott,K.A. and Hertzberg, A, "High Velocity Modes of the Thermally Choked Ram Accelerator," AIAA Paper 88-2925, July 1988

3. Bogdanoff, D.W., Knowlen, C., Murakami, D., and Stonich, I., "A Magnetic Detector for Projectiles in Tubes," submitted to AIAA Journal.

4. Griffiths, David J., Introduction to Electrodynamics, (Prentice-Hall, Inc., 1981), pp. 210-220, 235.

5. Jackson,J.D., Classical Electrodynamics, 2nd ed., (Prentice-Hall, Inc., 1975), pp. 217-220.

6. Peckner, Donald, Bernstein, I.M., Handbook of Stainless Steel, (McGraw-Hill Book Company, 1977), pp. 4-31.

7. Popov E.P., Mechanics of Materials, 2nd ed., (Prentice-Hall, Inc., 1978), pp. 275-295.

8. Wangsness, Roald K., Electromagnetic Fields, 2nd ed., (John Wiley & Sons, 1986), pp. 297-300, 382-383.